論文 / 著書情報
Article / Book Information

論題(和文)	
Title(English)	Effect of yield function ' s form on performance of the backward-Euler stress update algorithm for the original cam-clay model
著者(和文)	KHOSRAVI M.HOSSEIN, ピパットポンサー ティラポン
Authors(English)	M. H. Khosravi, T. Pipatpongsa, S. Kanazawa, A. Iizuka
出典(和文)	, , , pp. 161-164
Citation(English)	Proceedings of the 11th International Summer Symposium, JSCE, , , pp. 161-164
発行日 / Pub. date	2009, 9
権利情報 / Copyright	本著作物の著作権は土木学会に帰属します。 Copyright (c) 2009 Japan Society of Civil Engineers.

EFFECT OF YIELD FUNCTION'S FORM ON PERFORMANCE OF THE BACKWARD-EULER STRESS UPDATE ALGORITHM FOR THE ORIGINAL CAM-CLAY MODEL

M. H. Khosravi[1)] T. Pipatpongsa[2)]
S.Kanazawa[3)], A. Iizuka[4)]

1) Tokyo Institute of Technology, 2-12-1 O-okayama, Meguro-ku, Tokyo, Japan
E-mail: khosravi.m.aa@m.titech.ac.jp, 2) Ditto, E-mail: pthira@gsic.titech.ac.jp
3) Kobe University, 1-1 Rokkodai-cho, Nada-ku, Kobe 657-8501
E-mail: kanazawa@stu.kobe-u.ac.jp, 4) Ditto, E-mail: iizuka@kobe-u.ac.jp

INTRODUCTION

The original Cam-clay (Roscoe & Schofield, 1963) is the earliest constitutive equation with the simplest formulation in critical state soil model. However, it was later replaced by the modified version five years later due to some disadvantages. One of the drawbacks is the pierce corner (see Fig.1) existed on the yield surface. The corner represents the virgin consolidation history for the model but evaluation of plastic flow at this vertex singularity causes numerical trouble when the associated flow rule is applied. The isotropic mechanism of the model does not smoothly enclose the yield function thus the model is considered classical and academics, not practical. Nevertheless, basic researches and advanced applications of the original Cam-clay model are extensively developed in Japan. Integration of the rate constitutive equation has been implemented to Backward-Euler scheme in order to obtain more accurate, stable and robust algorithm (Yatomi & Suzuki, 2001). Also, it was found that Koiter's associated flow rule (Koiter, 1953) can provide mathematical treatment to the discontinuous gradient (Pipatpongsa et al., 2002). Based on the theoretical framework proposed by Simo, Kennedy & Govindjee (1988), Backward-Euler integration scheme for the original Cam-clay model is recently developed by the authors (Pipatpongsa et al., 2009) using the constraint condition to close the vertex (see Fig.1). The authors realize that success and fail of this development is also depended on the selection of yield function's form. The improper forms can lead to a poor algorithm which adversely deteriorates the robustness or ability to quickly capture the convergence.

In this study, four diversified forms of the yield function are listed in Table 1. All of them represent the similar function when equating to zero, i.e. $f_2=f_1/p$, $f_3=p_c(\exp(f_2)-1)$, $f_4=f_3/p$. Selection of the most appropriate form employed to the stress update algorithm is the objectives of this study. The description of the model and algorithm is briefly introduced. Through this study, we will refer the yield function to f when expressing collectively and to f with a numbering subscript when expressing individually. Because of $p\leq p_c$, elastic state is bounded by f. The typical expression and consistency condition of f are written by,

$$f = f(p,q,p_c) = 0\,. \tag{1}$$

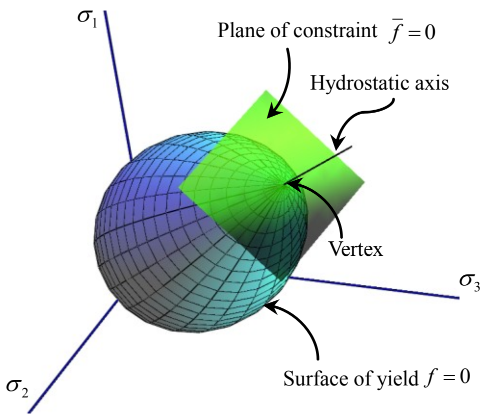

Figure 1: The original Cam-clay yield and the constraint functions in principal stress space

Table 1: Various forms of yield function diversified from the original Cam-clay (1963)

Forms	Types
$f_1 = p\ln(p/p_c)+q/M$	Logarithmic stress function
$f_2 = \ln(p/p_c)+q/Mp$	Logarithmic stress ratio function
$f_3 = p\exp(q/Mp)-p_c$	Exponential stress function
$f_4 = \exp(q/Mp)-p_c/p$	Exponential stress ratio function

Note: M is a critical state frictional parameter, p is a mean stress, p_c is an isotropic hardening stress parameter and q is a deviatoric stress. All stresses considered are effective stresses.
Remark: f_1 type are found in Yatomi & Suzuki (2001), f_2 type are found in Pipatpongsa et al. (2002), f_3 and f_4 are seldom employed but formulated for comparison purpose

MODEL DESCRIPTION

The constraint function is defined in addition to the regular yield function (Pipatpongsa et al., 2009).

$$\bar{f} = \bar{f}(p, p_c) = p - p_c = 0 \qquad (2)$$

where evolution of p_c is related to change of volumetric plastic strain $\varepsilon^p{}_v$ during loading conditions hence increasing for hardening and decreasing for softening responses. Elastic and plastic parts of strains are denoted by superscript e and p respectively

$$\Delta p_c / p_c = \Delta\varepsilon_v^p \left(1+e_o\right) / \left(\lambda - \kappa\right). \qquad (3)$$

where λ is a compression index, κ is a swelling index and initial void ratio is e_o. Koiter's associated flow rule combines two distinct plastic flows from mechanisms of regular yield and constraint functions using consistency parameters $\Delta\gamma$ and $\Delta\bar{\gamma}$. Variables with upper bar correspond to the constraint function.

$$\Delta\varepsilon_v^p = \Delta\gamma \frac{\partial f}{\partial p} + \Delta\bar{\gamma}\frac{\partial \bar{f}}{\partial p}, \quad \Delta\varepsilon_s^p = \Delta\gamma \frac{\partial f}{\partial q} + \Delta\bar{\gamma}\frac{\partial \bar{f}}{\partial q} \qquad (4)$$

Volumetric and deviatoric strain components are denoted by subscript v and s respectively. Elastic strains can be obtained by driving strains $\Delta\varepsilon_v$ and $\Delta\varepsilon_s$ as follow

$$\Delta\varepsilon_v^e = \Delta\varepsilon_v - \Delta\varepsilon_v^p, \quad \Delta\varepsilon_s^e = \Delta\varepsilon_s - \Delta\varepsilon_s^p. \qquad (5)$$

Nonlinear stress-strain relations are described by

$$\Delta p = K(p)\Delta\varepsilon_v^e, \quad \Delta q = 3G(p)\Delta\varepsilon_s^e, \qquad (6)$$

where pressure-dependent bulk moduli K and shear moduli G are obtained by

$$K(p) = \frac{1+e_o}{\kappa} p, \quad G(p) = \frac{3\left(1-2\nu\right)}{2\left(1+\nu\right)} K(p). \qquad (7)$$

where ν is a Poisson's ratio. According to Eqs.(6)-(7), the closed-form integration of nonlinear p and q can be given with the corresponding derivatives with strains (see Box.1). In addition to the yield functions shown in Eqs.(1)-(2), substitution of Eq.(4) to (5) formulates the residual functions $\tilde{\mathbf{r}}$ of state variables $\tilde{\mathbf{x}}$ which are composed of ε_v^e, ε_s^e $\Delta\gamma$ (and $\Delta\bar{\gamma}$). Unlike Forward-Euler, Backward-Euler scheme strictly require that for unloading/elastic loading processes, $f < 0$ and $\bar{f} < 0$, for the regular plastic loadings, $f = 0$ and $\bar{f} < 0$, while the corner loadings enforce both $f = 0$ and $\bar{f} = 0$. Therefore, there are three possible modes of solution controlled by $\Delta\gamma$ and $\Delta\bar{\gamma}$. The value of $\tilde{\mathbf{x}}$ is iteratively updated until $\left\|\tilde{\mathbf{r}}(\tilde{\mathbf{x}})\right\| < \Theta$ is converged. Θ is a numerical tolerance which is set to 10^{-5} in this study. Description of $\tilde{\mathbf{r}}(\tilde{\mathbf{x}})$, $\tilde{\mathbf{x}}$ and the trialed value $\tilde{\mathbf{x}}^{tr}$ are shown in Box 1. These nonlinear coupled systems in according to different forms of f are solved by Newton method with restart algorithm (see Figs.2-3). The variables with subscript i denote the initial values.

$$\tilde{\mathbf{x}} = \tilde{\mathbf{x}} - \partial_{\tilde{\mathbf{x}}}\tilde{\mathbf{r}}(\tilde{\mathbf{x}})^{-1} \cdot \tilde{\mathbf{r}}(\tilde{\mathbf{x}}) \qquad (8)$$

Box 1. Relevant variables and derivatives

1. Mean stress and deviatoric stress

$$p = p_i \exp\left(\frac{\varepsilon_v^e - \varepsilon_{vi}^e}{\kappa/\left(1+e_o\right)}\right) \quad \text{where} \quad \mu = \frac{3\left(1-2\nu\right)}{2\left(1+\nu\right)},$$

$$q = \begin{cases} q_i + 3\mu \dfrac{p_i}{\kappa/\left(1+e_o\right)}\left(\varepsilon_s^e - \varepsilon_{si}^e\right) & \text{if } \varepsilon_v^e = \varepsilon_{vi}^e \\ q_i + 3\mu \dfrac{p - p_i}{\varepsilon_v^e - \varepsilon_{vi}^e}\left(\varepsilon_s^e - \varepsilon_{si}^e\right) & \text{otherwise} \end{cases}$$

2. Stress hardening parameter

$$p_c = p_{ci} \exp\left(\frac{\varepsilon_v - \varepsilon_v^e - \varepsilon_{vi}^p}{\left(\lambda-\kappa\right)/\left(1+e_o\right)}\right)$$

3. Derivatives of stress variables

$$\partial p / \partial\varepsilon_v^e = p\left(1+e_o\right)/\kappa,$$

$$\frac{\partial q}{\partial \varepsilon_s^e} = \begin{cases} 3\mu \dfrac{p_i}{\kappa/\left(1+e_o\right)} & \text{if } \varepsilon_v^e = \varepsilon_{vi}^e \\ 3\mu \dfrac{p - p_i}{\varepsilon_v^e - \varepsilon_{vi}^e} & \text{otherwise} \end{cases},$$

$$\frac{\partial q}{\partial \varepsilon_v^e} = \begin{cases} 0 & \text{if } \varepsilon_v^e = \varepsilon_{vi}^e \\ 3\mu \dfrac{\varepsilon_s^e - \varepsilon_{si}^e}{\varepsilon_v^e - \varepsilon_{vi}^e}\left(\dfrac{\partial p}{\partial \varepsilon_v^e} - \dfrac{p - p_i}{\varepsilon_v^e - \varepsilon_{vi}^e}\right) & \text{otherwise} \end{cases}$$

4. Derivatives of stress hardening parameter

$$\partial p_c / \partial\varepsilon_v^p = \left(1+e_o\right)p_c/\left(\lambda-\kappa\right), \quad \partial\varepsilon_v^p/\partial\varepsilon_v^e = -1,$$

$$\partial p_c / \partial\varepsilon_v^e = -\left(1+e_o\right)p_c/\left(\lambda-\kappa\right)$$

5. State variables

regular: $\mathbf{x} = \left\{\varepsilon_v^e \quad \varepsilon_s^e \quad \Delta\gamma\right\}^T$,

corner: $\bar{\mathbf{x}} = \left\{\varepsilon_v^e \quad \varepsilon_s^e \quad \Delta\gamma \quad \Delta\bar{\gamma}\right\}^T$

6. Trial elastic states

$$\varepsilon_v^{tr} = \varepsilon_{vi}^e + \Delta\varepsilon_v, \quad \varepsilon_s^{tr} = \varepsilon_{si}^e + \Delta\varepsilon_s$$

$$p^{tr} = p(\varepsilon_v^{tr}), \quad q^{tr} = q(\varepsilon_v^{tr}, \varepsilon_s^{tr})$$

$$\mathbf{x}^{tr} = \left\{\varepsilon_v^{tr} \quad \varepsilon_s^{tr} \quad 0\right\}^T, \quad f^{tr} = f(p^{tr}, q^{tr}, p_{ci})$$

$$\bar{\mathbf{x}}^{tr} = \left\{\varepsilon_v^{tr} \quad \varepsilon_s^{tr} \quad 0 \quad 0\right\}^T, \quad \bar{f}^{tr} = \bar{f}(p^{tr}, p_{ci})$$

7. Residual functions

$$\text{regular: } \mathbf{r} = \begin{Bmatrix} \varepsilon_v^e - \varepsilon_v^{tr} + \Delta\gamma\,\partial f/\partial p \\ \varepsilon_s^e - \varepsilon_s^{tr} + \Delta\gamma\,\partial f/\partial q \\ f(p, q, p_c) \end{Bmatrix},$$

$$\text{corner: } \bar{\mathbf{r}} = \begin{Bmatrix} \varepsilon_v^e - \varepsilon_v^{tr} + \Delta\gamma\,\partial f/\partial p + \Delta\bar{\gamma}\,\partial \bar{f}/\partial p \\ \varepsilon_s^e - \varepsilon_s^{tr} + \Delta\gamma\,\partial f/\partial q \\ f(p, q, p_c) \\ \bar{f}(p, p_c) \end{Bmatrix}$$

Note: in general, $\tilde{\mathbf{x}}$ and $\tilde{\mathbf{r}}$ refers to both $\mathbf{x}, \mathbf{r}$ and $\bar{\mathbf{x}}, \bar{\mathbf{r}}$ collectively. Variables for corner mode are indicated by the upper bar

ALGORITHM OUTLINE

Basic properties of material shown in Table 2 are illustrated to validate the performance of the proposed algorithm. The certain strain increments are applied to test the algorithm for the initial stress located at the vertex. The magnitude of tested strains is normally taken by 5 times of characteristics strains (e.g. Simo et al., 1988). This amount is determined from the specific strain at initial yield stress to eliminate the effect of stress level. For the original Cam-clay model, volumetric and deviatoric characteristic strains, namely ε_{vy} and ε_{sy}, are considered at the pre-consolidated isotropic pressure p_{ci} and the corresponding critical envelope Mp_{ci} respectively. Formula and numeric values of characteristic strains are shown in Table 3.

Table 2. Material parameters and initial stresses

M	λ	κ	ν	e_o	p_i (kPa)	q_i (kPa)	p_{ci} (kPa)
1.00	0.10	0.02	0.20	2.00	100	0	100

Table 3. Material parameters and initial stresses

Characteristic strains	Formula	Numeric values
Volumetric	$\varepsilon_{vy} = \dfrac{p_{ci}}{K(p_{ci})} = \dfrac{\kappa}{1+e_o}$	0.667 %
Deviatoric	$\varepsilon_{sy} = \dfrac{Mp_{ci}}{3G(p_{ci})} = \dfrac{M}{3\mu}\dfrac{\kappa}{1+e_o}$	0.109 %

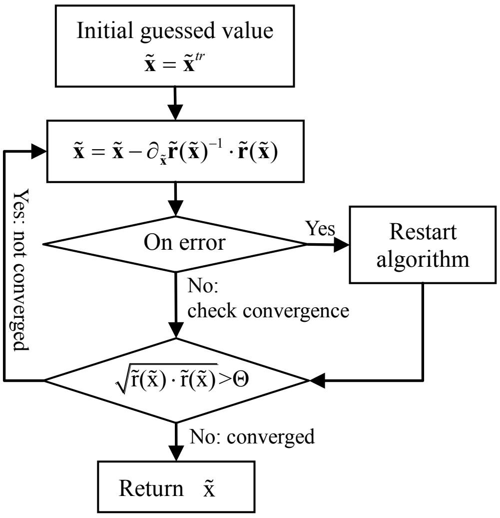

Figure 2: Newton method procedure

$$Err = \sqrt{\frac{3(p-p^*)^2 + 2/3(q-q^*)^2 + 3(p_c-p_c^*)^2}{3p^{*2} + 2/3q^{*2} + 3p_c^{*2}}} \quad (9)$$

According to the stress update algorithm shown in Fig.3, a trial stress is initially assumed to elastic state in order to judge the active surfaces in which yield criteria are violated. If both surfaces are active, the algorithm will initially assume corner mode. If $\Delta\bar{\gamma} < 0$ is found when the solution is converged, then the assumed mode of solution is corrected by moving to a regular mode.

PERFORMANCE EVALUATION

Iteration and error maps for different functions of the original Cam-clay model under the developed algorithm are constructed to obtain the contour map generated by a series of single-step strain increments imposed to the particular stresses on yield surface. The maximum error is found about 7% in the vicinity of the critical state, reflecting a high accuracy despite of a single large stress jump. Iteration maps for functions f_1 to f_4 are shown in Figs.5(a)-(d) orderly and digested to Table 4 for comparison. The overall accuracy is relatively evaluated from the exact solutions of the updated stresses. The exact solutions are obtained numerically by taking further repeatedly sub-division until there is no significant change.

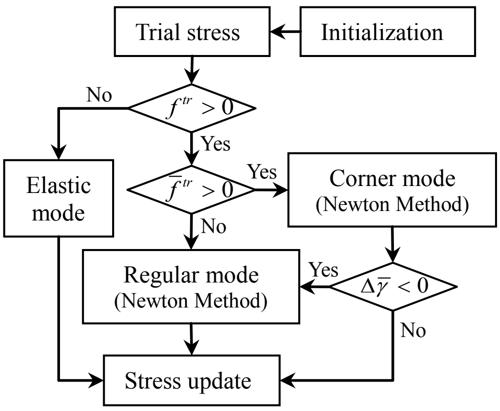

Figure 3: Stress update algorithm

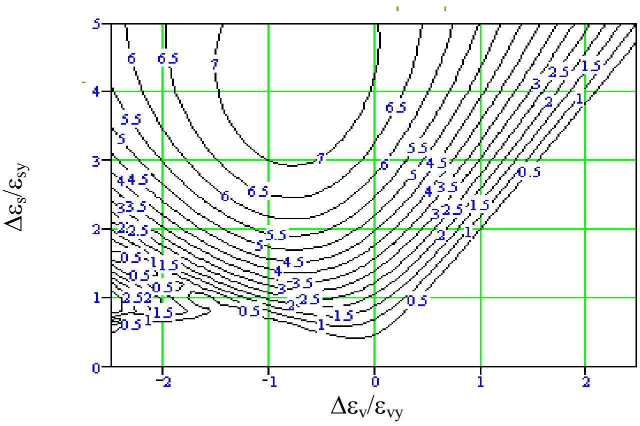

Figure 4: Percentage error-map contour

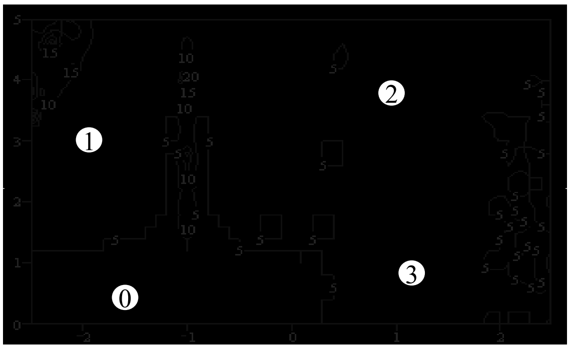

(a) Number of iteration based on f_1

(b) Number of iteration based on f_2

(c) Number of iteration based on f_3

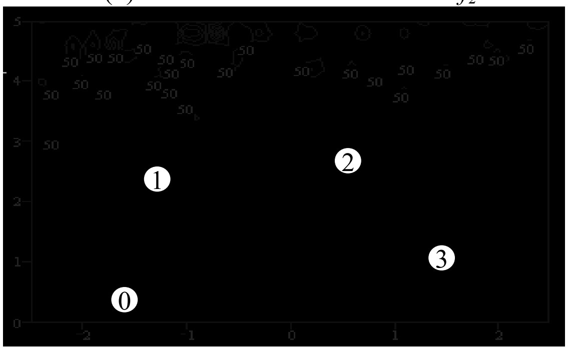

(d) Number of iteration based on f_4

Figure 5: Contours of iteration number for single step solution for various forms of yield function are plotted in the normalized strain space. The horizontal and vertical axes indicate the range of applied strains which are $\Delta\varepsilon_v/\varepsilon_{vy}$ and $\Delta\varepsilon_s/\varepsilon_{sy}$ respectively. Regions of four modes remarked by 0=elastic mode, 1=direct regular mode, 2=indirect regular mode and 3=corner mode are overlaid on the contours.

Four choices of yield function evaluated in this study give the same error maps as shown in Fig. 4. The considered domain of applied strain is 50 equal intervals of ±2.5 of $\Delta\varepsilon_v/\varepsilon_{vy}$ and 25 equal intervals of 0-5 of $\Delta\varepsilon_s/\varepsilon_{sy}$. Relative error is calculated by Eq.(9) where p^*, q^* and p_c^* are the exact stress solutions.

CONCLUSIONS

We found that form 1 (logarithmic stress function) shows the smallest numbers for both average and maximum iteration, hence indicating the most robust form. Because the iterative numerical scheme is linearized by Newton method, iteration number is relevant to the non-linearity degree and the discrepancy of the trialed values. Moreover, any attempt to diversification to the yield function may unintentionally induce more roots to the solutions.

Table 4. Robustness criteria of yield function

Forms	Avg. iteration no.	STD	Max. iteration no.
f_1	5.5	2.4	31
f_2	9.8	8.1	85
f_3	9.3	9.1	109
f_4	16.5	19.0	270

REFERENCES

Koiter, W.T., Stress-strain relations, uniqueness and variational theorems for elastic-plastic materials with a singular yield surface. Quart. Appl. Math., 1953, 11: 350-354.

Pipatpongsa, T., Iizuka, A., Kobayashi, I. & Ohta, H., FEM formulation for analysis of soil constitutive model with a corner in the yield surface, J. Structural Engineering Vol.48A, JSCE, pp.185-194, 2002

Pipatpongsa, T., Khosravi, M.H. & Ohta, H., Backward-Euler stress update algorithm for the original Cam-clay model with the vertex singularity, IS-Kyoto, Japan, 2009, pp. 179-185.

Roscoe, K.H., Schofield, A.N. & Thurairajah, A., Yielding of clays in state wetter than critical. Geotechnique, 1963, 13, 3: 211-240.

Simo, J.C., Kennedy, J.G. & Govindjee, S., Non-smooth multisurface plasticity and viscoplasticity Loading /unloading conditions and numerical algorithms. Int. J. Numer. Methods Engrg, 1988, 26: 2161-2185.

Yatomi, C. & Suzuki, Y., Finite element method analysis of soil/water coupling problems using implicit elasto-plastic calculation algorithm, JSCE Journal of Applied Mechanics, 2001, 4: 345-356.